

Data Rate vs. Maximum Reach in a Data Center Interconnect Scenario Exploiting Wideband InP Mach-Zehnder Modulators

Original

Data Rate vs. Maximum Reach in a Data Center Interconnect Scenario Exploiting Wideband InP Mach-Zehnder Modulators / D'Ingillo, Rocco; Borraccini, Giacomo; Virgillito, Emanuele; Straullu, Stefano; Siano, Rocco; Belmonte, Michele; Curri, Vittorio. - ELETTRONICO. - 2023-July:(2023), pp. 1-4. (Intervento presentato al convegno 2023 23rd International Conference on Transparent Optical Networks (ICTON) tenutosi a Bucharest, Romania nel 02-06 July 2023) [10.1109/ICTON59386.2023.10207487].

Availability:

This version is available at: 11583/2981801 since: 2023-09-12T14:04:24Z

Publisher:

IEEE

Published

DOI:10.1109/ICTON59386.2023.10207487

Terms of use:

This article is made available under terms and conditions as specified in the corresponding bibliographic description in the repository

Publisher copyright

IEEE postprint/Author's Accepted Manuscript

©2023 IEEE. Personal use of this material is permitted. Permission from IEEE must be obtained for all other uses, in any current or future media, including reprinting/republishing this material for advertising or promotional purposes, creating new collecting works, for resale or lists, or reuse of any copyrighted component of this work in other works.

(Article begins on next page)

Data Rate vs. Maximum Reach in a Data Center Interconnect Scenario Exploiting Wideband InP Mach-Zehnder Modulators

Rocco D'Ingillo^{1*}, Giacomo Borraccini¹, Emanuele Virgillito¹,
Stefano Straullu², Rocco Siano³, Michele Belmonte³, and Vittorio Curri¹

¹Politecnico di Torino, Turin, Italy; ²LINKS Foundation, Turin, Italy; ³Lumentum, Milan, Italy

Abstract: A new Mach-Zehnder DP-IQ ultra-wideband indium phosphide modulator with integrated optical semiconductor amplifiers has been characterized for time domain simulations to investigate data rate versus maximum range in a DCI scenario.

© 2023 The Author(s)

1. Introduction

Technological advancements in photonic integrated circuits (PICs) are significantly affecting the optical communications market; in particular, innovations in indium phosphide (InP) technology will provide semiconductors that may be used in integrated electro-optical Mach-Zehnder modulators (MZM) [1]. The unique features of the InP substrate additionally permit the integration of a laser source and semiconductor optical amplifiers (SOAs) on the same PIC. Furthermore, exponential increases in worldwide traffic demands produce a need for low power and low cost solutions for the 80–120 km optical links used in Data Center Interconnects (DCI) [2]. One promising SOA application with this built-in modulator integration is that coherent optical transmission at a high symbol rate is permitted, avoiding use of Erbium Doped Fiber Amplifiers (EDFAs) as booster amplifiers at the transmitter side of the optical link, allowing promising solutions for short-reach and Data Center Interconnect (DCI) applications [3]. For this reason, the goal of this work is to investigate the impact of integrated SOAs within an ultra-wideband (UWB) InP IQ-MZM PIC on a single-span, short reach optical link, for DCI applications. To properly observe the effect of this component on transmission, a characterization of an InP MZM sample with integrated SOAs has been performed for high data rate applications. The device characterization has been successively inserted in an accurate time-domain simulator to emulate a DCI scenario, testing different transmission conditions on a single span, short reach optical link. In this perspective, bit error rate (BER) and bit rate vs. maximum reach curves have been obtained and results are discussed, focusing on the advantages of SOAs on short reach transmission.

2. Experimental Setup & Device Characterization

The device under investigation is an UWB dual polarization (DP) InP IQ-MZM sample provided by Lumentum presenting two integrated SOAs at the two terminals: the *Pre-SOA* at the input and the *Post-SOA* at the output of the modulator structure, giving one for each polarization branch, as shown in Fig. 1. To estimate the impact of the SOAs on transmission performance, a characterization of the component considering different SOA operating conditions has been performed, transmitting a single polarization, 16 QAM modulation format with a symbol rate of 32 GBd. The characterization was performed in laboratory, using a laser source with 13 dBm input power as a light source at the modulator optical input with three different channels under test near the borders and the middle of the C-band, at 191.5, 193.5 and 195.5 THz. For the 16 QAM modulation application, a PAM-4 signal with a symbol rate of 32 GBd has been generated by a high-speed digital-to-analog converter (DAC), to be applied to the I and Q branches of the MZM. In order to properly control the working point of the InP MZM sample, a Lumentum evaluation board has been adopted, setting the best values for SOA power control, internal voltages and the electrical driver gain of the modulator for each case under test. To check the validity of the set working point, a Teledyne Lecroy Optical Modulation Analyzer (OMA) has been used to observe the eye-diagram of the signals applied to the electrical input of the I and Q branches of the MZM, and to observe the quality of the constellation, as shown in Fig. 2. Measurements of the optical signal-to-noise ratio (OSNR) of the transmitter, the modulator output power, P_{out} , and the gain of the SOAs have been performed in back-to-back, exploiting an optical spectrum analyser for OSNR measurement and an optical power meter to evaluate P_{out} . To properly characterize the transmission behaviour of the SOAs, for each input laser wavelength under test, different couples of *Pre-SOA* and *Post-SOA* settings have been tested, independently sweeping the SOA control current from the minimum to the affordable maximum of the component, sweeping its gain. The OSNR and P_{out} have been measured, obtaining a gain profile for the SOAs, and the OSNR profile of the modulator, for each pair of *Pre-SOA* and *Post-SOA* settings under test.

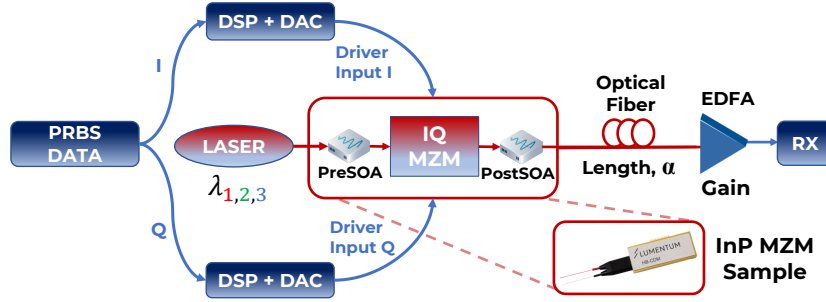


Fig. 1: Block scheme of the simulation framework.

3. Simulation Framework & Results

The simulation framework used for the investigation of the InP MZM behavior in a DCI scenario is shown in Fig. 1, including a time-domain simulator used as a quality of transmission (QoT) estimator [4], with a pseudo-random binary sequence (PRBS) data generator that produces a PRBS17 ($2^{17} - 1$ bits) sequence, split into two PAM- \sqrt{M} sequences (with M as the cardinality of the modulation under test) to be sent to the I and Q branches of the MZM, for both polarizations. The sequence is sent in input to a simulator module which acts as digital signal processing (DSP) and digital to analog converter (DAC) to produce a proper Nyquist shaped spectrum of the input digital signal. After the pulse is shaped, the signal is further processed by a custom low pass filter, obtained by characterization of the frequency response of the electrodes on the I and Q branches of the MZM sample under test, ensuring that the actual band-cut of the modulator sample is properly simulated. Three modulation formats have been simulated (DP-QPSK, DP-16 QAM, DP-64 QAM), at three different symbol rates (64, 96 and 128 GBd), in order to observe all significant use cases of the UWB InP IQ MZM, considering bit rates starting from 200 Gbit/s and going towards 1.2 Tbit/s. To generate the optical signal, a realistic laser light source has been modeled with 13 dBm as the input power, with 1 MHz of phase noise, centering the laser frequency at 191.5, 193.5 and 195.5 THz to emulate three different channels, $\lambda_{1,2,3}$, corresponding precisely to those used previously for the device characterization. The InP MZM has been simulated by starting from an analytical model of the MZM that also takes into account the non-linear phase response and absorption effect of a voltage-dependent transfer function of the InP modulator [5], properly setting the internal MZM parameters and its bias point to reproduce the component behavior via simulation [6]. The InP MZM simulation model has then been enhanced by including the SOA characterization, in order to observe the effect of the integrated amplification in transmission. Starting from the gain profiles for the *Pre-SOA* and *Post-SOA* pairs, we restricted our investigation to the three most significant SOA operating points, which are related to the minimum (*MIN*), maximum (*MAX*), and typical (*TYP*) SOAs working points. These are respectively related to the minimum and maximum affordable current control of the SOAs, and to the typical working point used in the linear region of SOA amplification, used to avoid potential distortion of the output amplified modulated signal. To correctly observe and isolate the effects of the described transmitter model, simulations have been performed without considering further impairments at

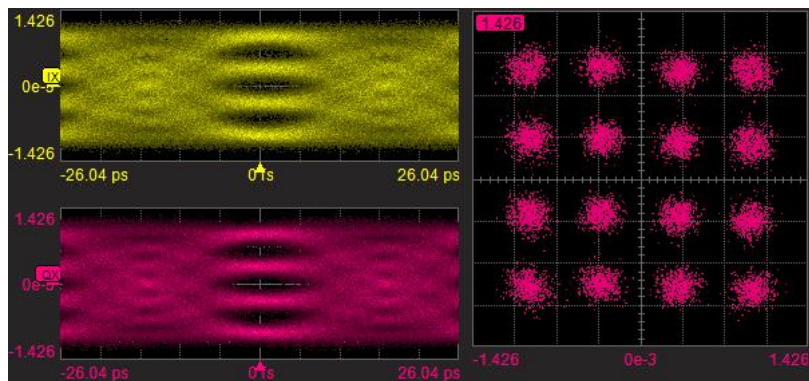


Fig. 2: OMA acquisition of eye-diagram and constellation of a 16 QAM signal at the output of the InP MZM, performed during modulator characterization.

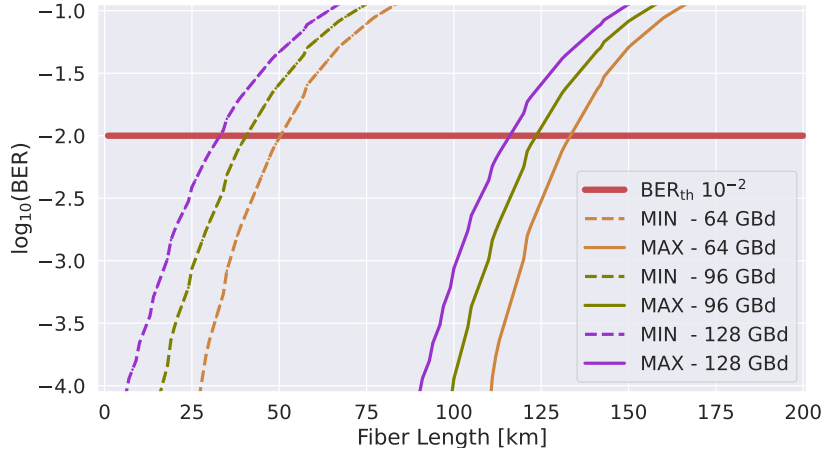


Fig. 3: \log_{10} (Pre-FEC BER) vs. Fiber Length [km] curves obtained by simulation, considering two SOA operating conditions (MIN and MAX), and three symbol rates (64, 96 and 128 GBd) for a DP-16 QAM modulation format, for a channel at 193.5 THz.

transmitter side, in order to investigate the maximum affordable limit for the system under test for the observed cases in the presented work. In order to simulate a DCI case, the optical signal at the output of the InP MZM is sent directly to an optical link, as shown in Fig. 1, without the presence of a booster EDFA. This optical link has been modeled by considering an optical fiber with an attenuation, α , of 0.2 dB/km, a variable length corresponding to that found within a DCI of 1–200 km, with a pre-amplifier EDFA at the receiver side with a variable gain in an affordable range for pre-amplifiers of 0–35 dB, and a typical noise figure value for pre-amplifier EDFAs of 5 dB. By considering the non-linear interference (NLI) noise in short-reach and DCI systems as negligible [7], and utilizing the additive white gaussian noise (AWGN) properties of the optical channel, it has been possible to treat all noise terms independently and separately in transmission [8]. As a result, the overall OSNR of the system can be obtained by modeling only two OSNR terms: $OSNR_{TX}$ measured during MZM characterization, related to the only InP MZM with integrated SOAs at transmitter side, and a simulated $OSNR_{RX}$, obtained by scaling EDFA gain increasing fiber length, in order to reach a minimum acceptable power threshold at the receiver side, $P_{RX,min}$, setting it to a typical value of -18 dBm corresponding to the value used when characterizing coherent optical pluggable transceivers. The simulations have been performed using a simulated constant-phase-estimator (CPE) aided coherent receiver, with bit error rate (BER) counting performed using DSP. From BER vs. OSNR results obtained through back-to-back simulations of the InP MZM, a BER threshold, BER_{th} , has also been set to 10^{-2} , in order to only take into account the signals with a lower BER and, consequently, a higher overall OSNR at receiver side. Testing all possible combinations of SOA configurations, modulation formats (MFs), symbol rates, R_S , and

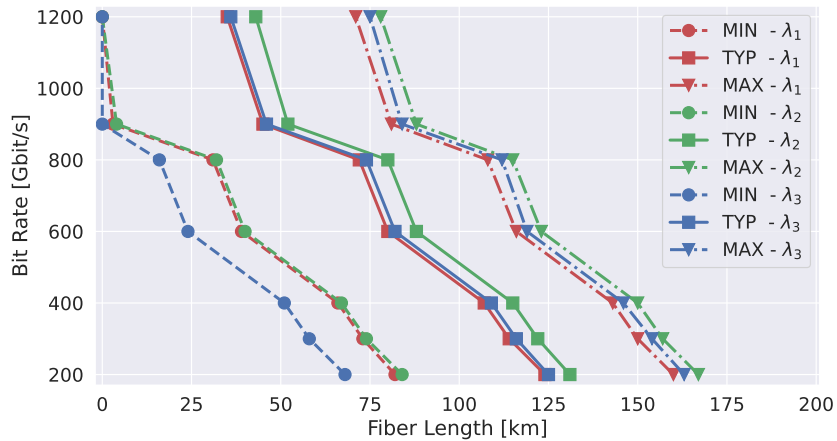


Fig. 4: Bit Rate [Gbit/s] vs. Fiber Length [km] obtained by simulation, considering three SOA operating conditions (MIN, TYP and MAX) for three wavelengths $\lambda_{1,2,3}$ under test, at 191.5, 193.5 and 195.5 THz, respectively.

Modulation Format	Symbol Rate [GBd]	Bit Rate (FEC-OH~28%) [Gbit/s]	Spectral Efficiency [bit/s/Hz]	Maximum Reach [km] @ SOA Minimum			Maximum Reach [km] @ SOA Typical			Maximum Reach [km] @ SOA Maximum		
				@ λ_1	@ λ_2	@ λ_3	@ λ_1	@ λ_2	@ λ_3	@ λ_1	@ λ_2	@ λ_3
				DP-QPSK	64	200	3.125	82	84	68	124	131
	96	300	3.125	73	74	58	114	122	116	150	157	154
	128	400	3.125	66	67	51	107	115	109	143	150	146
DP-16 QAM	64	400	6.25	48	49	33	89	97	91	125	132	129
	96	600	6.25	39	40	24	80	88	82	116	123	119
	128	800	6.25	31	32	16	72	80	74	108	115	112
DP-64 QAM	64	600	9.375	15	16	0	56	64	58	92	99	96
	96	900	9.375	3	4	0	45	52	46	81	88	84
	128	1200	9.375	0	0	0	35	43	36	71	78	75

Table 1: Maximum Reach [km] vs. Bit Rate [Gbit/s] scaled of FEC-OH~28% simulation results considering three modulation formats (QPSK, 16 QAM, 64 QAM) in polarization multiplexing, for three different symbol rates (32, 64, 96 GBd), three SOAs operating configurations (*MIN*, *TYP*, *MAX*), for three wavelengths ($\lambda_{1,2,3}$) under test at 191.5, 193.5 and 195.5 THz.

channel wavelengths, λ_i , the maximum reach L_{MAX} of the optical fiber has been found for each case under test, giving the results presented in Tab. 1. In Fig. 3 results related to *MIN* and *MAX* SOA settings for a DP-16 QAM modulation format are shown, providing \log_{10} (Pre-FEC BER) vs fiber length curves obtained via simulation for all considered R_S values, focusing on a specific case with a single λ_2 channel with a DP-16 QAM modulation format. It can be observed that, under the same applied modulation conditions, the maximum feasible reach to obtain a BER lower than BER_{th} is critically improved by setting the SOA operating points to *MAX*, obtaining an improvement of ≈ 80 km for each case under test. In Fig. 4 bit-rate vs. maximum reach simulation results are shown, taking into account all SOA settings and wavelengths under investigation. Additionally, in this case the represented bit rate trend is substantially improved by setting the SOA to *MAX*. In particular, Fig. 4 and Tab. 1 show that the maximum affordable bit rate (already scaled with respect to a typical FEC overhead (FEC-OH) of 28%) for a typical DCI optical link of 80 km is 200 Gbit/s for the SOAs set to *MIN*, and it is greatly improved to 1.2 Tbit/s by setting the SOAs at *MAX* and by using a DP-64QAM modulation format at 128 GBd. Importantly, in Tab. 1 it can be observed that the best wavelength choice is λ_2 , (which lies in the center of the C-band) with a maximum reach of 167 km for 200 Gbit/s solutions and 78 km for a 1.2 Tbit/s case. These results show that the InP MZM with integrated SOAs can be considered as a strong candidate for DCI and short reach applications.

4. Conclusion

A performance investigation of an UWB InP DP-IQ MZM with integrated SOAs in a DCI scenario is presented, focusing on time-domain simulations of the component under different operating conditions. To ensure accurate modeling of this component, device characterization has been performed in a laboratory set-up and embedded into the simulation framework. The results of the simulation show that InP MZMs with integrated SOAs are promising candidates for DCI solutions in terms of bit rate and maximum affordable reach.

Acknowledgment

This research activity has been made possible thanks to valuable contributions by Links Foundation and Lumentum.

References

1. Meint Smit et al. "Past, present, and future of InP-based photonic integration", APL, 2019.
2. M. H. Eiselt, "Data Center Interconnects at 400G and Beyond", OECC, 2018.
3. H. Zhao et al., "High-Power Indium Phosphide Photonic Integrated Circuits", IEEE Journal of Selected Topics in Quantum Electronics, 2019.
4. A. D'Amico et al., "Quality of Transmission Estimation for Planning of Disaggregated Optical Networks", ONDM, 2020.
5. R. A. Griffin et al. "InP Mach-Zehnder Modulator Platform for 10/40/100/200-Gb/s Operation" in IEEE Journal of Selected Topics in Quantum Electronics, vol. 19, 2013.
6. R. D'Ingillo et al., "Simulative Analysis of InP-based Dual Polarization IQ Mach-Zehnder Modulators", ACP, 2022.
7. T. Mano et al., "Accuracy of Nonlinear Interference Estimation on Launch Power Optimization in Short-Reach Systems with Field Trial", ECOC, 2022.
8. V. Curri, "Software-Defined WDM Optical Transport in Disaggregated Open Optical Networks" ICTON, 2020.